

# The Laboratory Evaluation of the Heating Mode Part-Load Operation of an Air-to-Air Heat Pump

W.A. Miller, P.E.

ASHRAE Associate Member

## ABSTRACT

The laboratory evaluation of the part-load Coefficient of Performance (COP) and capacity of an air-to-air heat pump were conducted in a parametric study of heat pump on-time, off-time, and outdoor ambient temperature. A split-system heat pump was instrumented and tested in the heating mode to gain better understanding of the physical processes of the cycling phenomena that degrade heat pump COP and capacity.

Improvement in cycling COP and capacity was observed by controlling off-cycle refrigerant migration. Best cycling COP and capacity performance occurred for cycling tests conducted with refrigerant isolated in the indoor heat exchanger during the off-cycle, coupled with 2 min of extended indoor blower operating during the off-cycle.

The analysis of loss per on and off cycle revealed refrigerant dynamics to cause appreciable time delays in establishing steady-state heat pump COP.

## INTRODUCTION

Cycling operation of a vapor compression heat pump results in degradations of Coefficient of Performance (COP) and capacity. Cycling is responsible for the major losses in heat pump efficiency yet detailed information on cycling is sparse. Studies conducted by Kelly and Parken (1977), Tanaka (1982), Mulroy and Didion (1983), and Murphy and Goldschmidt (1984) have addressed qualitatively the refrigerant pressure, temperature, and efficiency trends observed during on and off cycling transients. Mulroy investigated the movement of refrigerant within a heat pump system during cooling mode tests having a 6-min-on and 24-min-off cycling rate. Tanaka analyzed the refrigerant dynamics of a heat pump system operating in the two different modes: (1) heat pump energized to equilibrium after being off for 16 hours; (2) heat pump energized after previous history of a 60-min-on period and a 10-min-off period. Both Mulroy's and Tanaka's studies clearly showed the importance of heat pump refrigerant dynamics in explaining the cycling phenomenon.

Reported here are the results of single-speed cycling tests conducted on a nominal three-ton, split-system air-to-air heat pump. Parameters varied in the study include heat pump on-time, off-time, and outdoor ambient temperature. Continuous measurements of the weight of refrigerant within the outdoor unit were made during both on and off periods of a cycle for further information on the cycling process. Cycling tests were conducted on the heat pump in the following modes:

1. Continuous indoor blower operation with compressor and outdoor fan cycling on and off,
2. Compressor, indoor blower, and outdoor fan cycling on and off, termed normal cycling operation,
3. Indoor blower operation extended into off cycle with compressor and outdoor fan cycling on and off,
4. Refrigerant isolated in indoor coil during off cycle with system operating in normal cycling mode,\* and
5. Off cycle refrigerant isolation in the indoor coil and extended indoor blower operation with compressor and outdoor fan cycling on and off.

\* Compressor, indoor blower, and outdoor fan cycle off during off cycle.

W. A. Miller is employed by the Energy Division of Oak Ridge National Laboratory, Oak Ridge, Tennessee.

Results of cycling tests conducted on the heat pump operating in the above modes are presented together with the fraction of cycling losses caused by thermal losses from the indoor coil and refrigerant dynamic losses during the on period of a cycle.

## LABORATORY FACILITY

### Heat Pump

A split-system air-to-air heat pump was selected for the study. The heat pump refrigerant circuit is similar to conventional design for a split-system, air-to-air, single-speed heat pump. Liquid refrigerant is throttled by capillary tubes in both the cooling and heating modes. Both indoor and outdoor heat exchangers are of tube and plate fin configuration. A liquid line to suction line heat exchanger heats refrigerant before it enters the compressor housing, and the heat pump has a suction line accumulator to protect the compressor.

### Test Stand

The cycling tests were conducted in adjacent environmental chambers with temperature and humidity control. Department of Energy (DOE) cycling test tolerances specified in the Federal Register (1979) were observed to enable some comparison to manufacturers data.

The heat pump was instrumented with 64 thermal ribbon platinum resistance temperature detectors (RTD) for measuring both heat exchanger wall temperatures and refrigerant circuit temperatures. All RTD's were calibrated in situ and observed to have accuracies of  $\pm 0.5F$  ( $0.3^{\circ}C$ ). The response time of the thermal ribbon RTD was measured to be approximately 5 sec for a  $30F^{\circ}$  ( $17C^{\circ}$ ) step change in temperature. Refrigerant pressures were measured at inlet and outlet of the compressor and heat exchangers using bellows-actuated force-balance transducers. The pressure transducers were observed to have accuracies of  $\pm 1\%$  of reading or better. Single-phase refrigerant mass flow rate was measured in the liquid line using a mass flow meter.\*

The migration of refrigerant entering or leaving the outdoor unit was measured using a weight scale incorporating a counterbalance as shown in Figure 1. In situ calibrations were made to ensure that the counterbalance would act as the tare weight (weight of outdoor unit without a refrigerant charge). A load cell, mounted in cantilever beam configuration, and a micrometer, Figure 1, were then adjusted and fixed for later measurements of refrigerant weight within the outdoor unit. Vertical thrusts in the liquid and vapor line were eliminated by using flexible couplings between outdoor housing and the vapor and liquid line. Accuracy of the weighing system was checked while the heat pump operated in heating mode, and was observed to be  $\pm 0.1$  lb (0.22 kg). Time response of the refrigerant weighing system was approximately 15 when subjected to a 2.2 lb (1.0 kg) step change in weight.

The air-side indoor heat exchanger capacity was measured using a thermopile grid comprised of thirty-junctions connected in a series combination of 24 AWG copper constantan wire and a duct airflow measuring device (multipoint pitot tube averaging traverse).

Compressor power, indoor blower, and outdoor fan power were measured with power transducers having accuracies of 2% of reading.

All temperature, pressure, power, flow, and refrigerant weight measurements were monitored by a data acquisition system (DAS) and a PDP-11 host computer. The computer system as coupled to the analog subsystem has capability of both monitoring and controlling 50 channels per second.

---

\* Refrigerant flows through a U-shaped flow tube that vibrates as a tuning fork. The transducer detects a coriolis or gyroscopic force associated with moving fluid particles that is directly proportional to mass flow rate.

## EXPERIMENTAL PROCEDURE

### Steady State

The heat pump was operated for a period of two hours inside the controlled ambient temperature and humidity conditions of the environmental chambers prior to steady-state data collection. Temperatures and pressures in the refrigerant circuit, power consumption, and capacity of the heat pump were monitored for observation of established heat pump steady-state operation. On command, the DAS and host computer then monitored refrigerant-side and air-side data at 10 sec intervals over a period of one hour

for use in calculating average COP and capacity. Calculated values of heat pump COP and capacity based on air-side measurements were within 3% of calculated values based on refrigerant-side measurements.

### Cycling Test

A series of cycling tests were conducted by varying one of three parameters (on time, off time, or outdoor temperature) while holding the other two parameters fixed. Experimental investigation of the effect of each parameter on cycling transients revealed its importance in cycling operation. The temperature and humidity of the environmental chambers were controlled to ensure sensible (dry coil) heat transfer for both indoor and outdoor heat exchangers. Control of the heat pump and data collection were performed automatically by the DAS and PDP-11 host computer system. Selections of heat pump on time, off time, cooling or heating mode, continuous indoor blower, and off-cycle refrigerant migration control were made interactively at the start of each cycling test. Repetitive cycling operation of the heat pump was established by automatically cycling the heat pump through three on and off cycles prior to data collection. Data on three to four cycles of heat pump operation were then collected and filed on the host computer.

Heat pump data were monitored at preset time intervals in each on- and off-period of a given cycle. As time progressed into each on- and off-period, the scan rate was automatically adjusted according to the severity of the time-dependent transients. After completing three to four heat pump data collection cycles, the heat pump was then cycled either on or off and allowed to establish equilibrium conditions. Heat exchanger wall temperatures, compressor housing temperatures, refrigerant pressures, and weight of the refrigerant in the outdoor unit were monitored for observation of system response in reaching steady-state conditions.

Collected data were accumulated to obtain averages of COP and capacity during cycling. This was done by superimposing the three to four cycles of heat pump data. Statistical error analysis was performed to determine the precision of individual data measurements within given time bins of superimposed on- and off-cycles per cycling test. The error analysis is based on a normal distribution and assumes a 95% probability that the mean value falls within two standard deviations of the true value.

### STEADY STATE RESULTS

Steady-state COP and capacity were observed to vary linearly with outdoor ambient temperatures ranging from 50F (10°C) to 30F (-1°C). The steady-state COP at 50F (10°C) outdoor temperature was 3.14, and the measured heating capacity was 37.8 kBtu/h (11.1 kW). At an ambient outdoor temperature of 30F (-1°C), the observed COP and capacity were 2.48 and 26.2 kBtu/h (7.7 kW) respectively.

The distribution of refrigerant charge was calculated from steady-state measurements of weight of refrigerant in the outdoor unit and is listed in Table 1. At 50F (10°C) outdoor temperature, the outdoor unit contained 34.2% of the total refrigerant charge,\* while calculations showed the indoor heat exchanger held 48.0% of the total charge. At the lower outdoor temperature of 30F (-1°C), the outdoor unit contained 53.7% of total charge and the indoor heat exchange held 29.0% of total charge. Results in Table 1 show the outdoor unit to contain 2.4 lb (1.1 kg) more refrigerant during the 30F (-1°C) steady-state test as compared to the 50F (10°C) steady-state test. The air-to-refrigerant temperature difference across the outdoor coil was measured as 17F (9.4°C) for the 50F (10°C) outdoor temperature test, while the air to refrigerant temperature difference decreased to 11F° (6C°) for the 30F (-1°C) outdoor temperature test. The reduction of temperature difference between outdoor air and refrigerant within the outdoor coil together with the reduced evaporator pressure decreases refrigerant density at inlet to the compressor. This, in turn, decreases the evaporator heat output and the mass flow rate pumped by the constant-volume reciprocating compressor. These reductions, observed as outdoor temperature drops, cause an increase in the amount of refrigerant stored in the accumulator.

\* The heat pump total charge was 12.5 lb (5.7 kg), being 4.4 lb (2 kg) more than nameplate charge because of added line lengths for instrumentation.

### CYCLING TEST RESULTS

System performance was observed for a broad range of cycling rates, including those that simulate field cycling rates observed by Baxter (1984). Baxter's field data revealed surprisingly low cooling mode cycling rates for a three ton heat pump controlled in separate field tests by thermostats designed for four and five cycles per hour (CPH) at 50 percent load. Laboratory cycling experiments therefore centered on heating mode operation for cycling rates that cover the range of observed field cycling rates.

Cycling COP is based on air-side measurements and is calculated using Equation 1. Off-cycle crankcase heater energy is not included unless otherwise specified.

$$COP_{cyc} = \frac{Q_{on} + Q_{off}}{E_{total}} \quad (1)$$

$Q_{on}$  = Integrated indoor coil heat output measured on the air-side during the on period,

$Q_{off}$  = Integrated indoor coil heat output measured on the air-side during the off period,

$E_{total}$  = Integrated energy consumption of compressor and fans during total cycle.

### Efficiency Loss Due to Cycling

The part-load factor (PLF), ratio of cycling COP to steady-state COP is plotted in Figure 2 as a function of the load factor, defined by Equation 2, for tests conducted at 50F (10°C) outdoor temperature. The solid curve in Figure 2 was developed by assuming the load factor (LF) to be related to percent on-time (on period/ $T_{cyc}$ ) by the ratio of the average cycling capacity rate to steady-state capacity. Here it is assumed that the house load is equivalent to the heat pump part-load output as defined by the control logic of the thermostat. Laboratory data of cycling COP were therefore fit to on and off periods that represent cycling rates for a thermostat model [cycles per hour (CPH) parabolic function of percent on-time] designed to have 3 CPH at 50% load. Thus the thermostat model was used to calculate on and off periods that were fit to actual test data shown by dotted lines in Figure 2. The solid curve therefore represents heat pump cycling COP as related to house load and cycling rate.

The coupling of part-load efficiency to house load was first developed by Parken and Kelly (1977). Their derivation assumes cycling rate to be dominated by thermostat dynamics and that the part load factor (PLF) is independent of outdoor temperature. Lamb and Tree (1981) conducted thermostat studies and verified Parken and Kelly's first assumption. Lamb and Tree concluded the switch differential\* and anticipator temperature rise\*\* had predominate effects on cycling rate.

$$LF = \frac{Q_{cyc} + Q_{off}}{Q_{ss}(T_{cyc})} \quad (2)$$

where

$Q_{ss}$  = steady-state capacity,

$T_{cyc}$  = period of the on and off cycle.

The family of dashed curves of constant on time in Figure 2 reveals the sharp decline in heat pump COP as on-time decreases from 50 min to 2-min for tests conducted at 50F (10°C) outdoor temperature. The solid curve, representing cycling COP as a function of load and cycling rate, displays COP degradations as load factor decreases. At 90% on time (50-min-on, 5.5-min-off) heating output was degraded 10.6% of steady-state capacity and COP was degraded 6.6% of steady-state COP. Results at 20% on time (6-min-on, 24-min-off) revealed a 34.5% reduction in heating output and a 29.6% reduction in steady-state COP.

Including the off cycle crankcase heater (40W) had little effect on performance except for load factors of less than 0.25. At a load factor of 0.13 (20% on-time), COP and capacity were reduced 32.9% and 35.0% of steady-state performance values, respectively.

**Cycling Phenomena.** Heat pump cycling trends are analyzed to gain insight to the underlying causes of cycling that result in the degradation of COP as seen in Figure 2. Off cycle and on cycle transients are discussed for cycling tests conducted at 50F (10°C) outdoor temperature having an 8-min-on and 30-min-off (21% on-time) cycling rate.

**Off-Cycle.** At the start of the 30 min off cycle, subcooled refrigerant was visually observed flowing through the liquid line for 45 sec during which 2.5 lb (1.6 kg) of refrigerant migrated to the outdoor unit. Refrigerant then began to flash as it discharged from the indoor coil for 5 min. during which roughly 94% of the total refrigerant migration occurred.

The migration of refrigerant caused indoor and outdoor heat exchanger temperatures to change roughly 20F° (11C°) within this 5 min interval, Figure 3. The rapid increase in outdoor coil wall temperature is the result of latent heat transfer from condensing refrigerant that migrated to the outdoor coil. Throughout the first 5 min of the off-cycle, refrigerant saturation temperature is observed in Figure 3 to be greater than outdoor coil wall temperature, resulting in refrigerant condensation within the outdoor coil. The refrigerant vapor that accumulates in the outdoor coil must condense to allow further migration. Thus the rate of migration is

\* Switch differential is the difference between cut-in and cut-out points measured at the thermostat under operating conditions.

\*\* Anticipator temperature rise is the number of degrees above ambient temperature that the anticipator adds to air within the thermostat cover.

governed by the heat exchanger wall temperature. Similar results were also observed by Murphy and Goldschmidt (1984). Both outdoor coil temperature and refrigerant pressure reach a maximum off cycle level, seen in Figure 3, that coincides in time with the majority of refrigerant migration. Once migration stops, system high-side and low-side pressures are observed in Figure 3 to have equalized; however, these pressures continue to drop together as the outdoor coil temperature equilibrates with the surrounding ambient temperature.

The accumulator wall temperature is plotted in Figure 4 as a function of time into the off-cycle. The Figure shows that refrigerant migration continues through the outdoor coil and into the accumulator and possibly the compressor. Little variation in the wall temperature of the accumulator was seen during the on-cycle; however, a definite temperature variation was observed along the height of the accumulator during the off-cycle, Figure 4. A maximum temperature variation occurred at roughly 6 min into the off-cycle and revealed the accumulator to be half full of liquid refrigerant. As time progressed into the off-cycle, refrigerant vapor condensed as seen by the decrease in wall temperature for the upper half of the accumulator. This refrigerant vapor migration to the accumulator and compressor is implied from temperature measurements; however, the amount of off-cycle migration to individual components cannot be determined from the data.

**On Cycle.** The migration of refrigerant during the off cycle results in start-up refrigerant dynamics that are crucial in terms of the cycling loss. The outdoor heat exchanger and accumulator, being half full of liquid refrigerant, hold the majority of migrated refrigerant in the outdoor unit just before system start-up. Within one min, the compressor pumps approximately 4.0 lb (1.8 kg) of refrigerant from system low-side to high-side as seen in Figure 5. A peak in compressor power is also indicated in Figure 5 at approximately 30 sec of operation because of a high density of saturated refrigerant vapor being pumped by the compressor. The saturated refrigerant conditions within the compressor housing are implied from a sharp drop in housing temperature measured at the compressor oil level.

As time progresses into the on-cycle, the evaporator pressure decreases as the compressor continues to pump refrigerant to the high-side. This drop in pressure causes a flashing of refrigerant in the evaporator which in turn drops outdoor coil wall temperature by 15F° (8.3°C), Figure 6. The indoor coil was calculated to hold only 0.5 lb (0.22 kg) of refrigerant vapor at start-up and therefore a high quality saturated mixture is throttled by the outdoor capillary for approximately 2 min of compressor operation. The mass flowrate through the liquid line is well below steady-state levels since the majority of refrigerant is still in the outdoor unit. The evaporator coil becomes starved for refrigerant and the accumulator, serving to protect the compressor, fills with liquid refrigerant [Mulroy and Didion (1985)]. These refrigerant dynamics around the accumulator and compressor cause the heat exchangers to be undercharged and result in the change in slope of cycling heat output as seen in Figure 5. The development of steady-state charge distribution is gradual after 2 min of compressor operation, Figure 5. This occurs because liquid refrigerant in the accumulator must be pumped through the orifice at the bottom of the accumulator U-tube (i.e. liquid refrigerant and oil return hole).

High-side refrigerant pressure and average indoor heat exchanger temperature, Figure 6, continue to increase until a steady-state refrigerant distribution is established after 10 min of heat pump operation. Steady-state COP and capacity were established at roughly 15 min of operation. However the compressor housing temperature does not equilibrate until 20 to 25 min of compressor operation as a result of the refrigerant dynamics observed around the accumulator and compressor at start-up.

### Effect of Outdoor Ambient Temperature

The COP and heating capacity of a heat pump are effected by outdoor heat exchanger capacity, which is a function of outdoor temperature. Steady-state and cycling COP decrease as outdoor temperature decreases; however, the ratio of cycling COP to steady-state COP increased with decreasing outdoor temperature. This inverse relationship of cycling COP ratio and outdoor temperature is caused by refrigerant density effects.

The solid curves of Figure 7, representing heat pump performance as related to load and cycling rate, display improvement in the ratio of cycling to steady-state COP as outdoor ambient temperature decreases from 50F (10°C) to 30F (-1°C).<sup>\*</sup> The COP and heating capacity observed at 50F (10°C) outdoor temperature and 90% on-time degraded 6.6% and 1.6% of steady-state value respectively, while at 30F (-1°C) outdoor temperature and 90% on-time COP and capacity degraded 4% and 6.7% respectively. Results at 20% on-time in Figure 7 show cycling performance as a function of outdoor temperature to be roughly equal. Cycling COP and capacity observed for both temperatures at 20% on-time were degraded by roughly 30% of steady-state COP and capacity.

Capacity, normalized to steady-state capacity, improved for cycling tests conducted at 21% on time (8-min-on and 30-min-off) as the outdoor temperature decreased from 50F (10°C) to 30F (-1°C), Figure 8. Normalized compressor power trends were similar for

<sup>\*</sup> Heat pump cycling would not be expected for outdoor temperatures such as 30F (-1.1°C) that would be below the house balance point. However, a broad temperature range was selected in these experiments to observe its effect on cycling dynamics.

the two outdoor temperature cycling tests; however, compressor start-up transients were less severe as seen in Figure 8 for the lower temperature test. Also steady-state compressor operation was established more rapidly at the lower temperature test.

Refrigerant weight as a function of compressor run time, displayed in Figure 9, reveals that 7.4 lb (3.4 kg) of refrigerant was pumped to the indoor coil and liquid line during the 8-min-on period of the 50F (10°C) cycling test. At 30F (-1°C) outdoor temperature, 5 lb (2.3 kg) of refrigerant was pumped from the outdoor unit during the 8-min-on period. The decrease in outdoor temperature causes evaporator pressure to decrease and thus lowers refrigerant density at compressor inlet. These reductions of refrigerant properties, in turn, decrease the pumping ability of the compressor, resulting in the 2.4 lb (1.1 kg) differential of refrigerant movement as function of outdoor temperature. Since more refrigerant is circulating throughout the system at 50F (10°C) outdoor temperature, the cycling losses will be greater due to the time required to boil-off refrigerant within the accumulator. A time lag of 12 min\*\* was observed in establishing near steady-state condensing and evaporating temperature and pressure for the 50F (10°C), 21% on-time cycling test. However, only 6 min were required to establish quasi-steady-state condensing and evaporating conditions for the 30F (-1°C) cycling test. Thus cycling losses decrease with decreasing outdoor temperature because less time is required to achieve proper system charge distribution as temperature decreases.

The dependence of part-load COP on outdoor temperature reveals that both duty-cycle and refrigerant dynamics cause more severe COP cycling degradations in the warmer months of the heating season as compared to the colder portion of the heating season. The result also shows that PLF as related to heating load and cycling rate to be dependent on outdoor temperature.

\* System allowed to cycle on to equilibrium after three previous 8-min-on and 30-min-off cycles.

### CYCLING CONTROL STRATEGIES

A series of heating mode cycling tests was conducted at 50F (10°C) outdoor temperature to measure system improvements resulting from the control strategies previously listed in the introduction. The part-load factor (PLF) is plotted in Figure 10 as a function of load factor (LF) for an indication of cycling efficiency resulting from these control strategies.

Best part-load efficiency was obtained by controlling off-cycle refrigerant migration and extending indoor blower operation by 2 min. At 68% on-time, COP and capacity degradations for off cycle refrigerant control and extended blower were 3.9% and 9.6% of steady-state as compared to normal mode\* cycling COP and capacity degradations of 16.9% and 28%. At 20% on-time, the part load factor (PLF) for off cycle migration control drops slightly below the PLF observed with 2 min of extended indoor blower operation as seen in Figure 10. During the off cycle of the refrigerant migration control cycling test, the isolation valves leaked roughly 2 lb. (0.9 kg) of refrigerant. The off cycle refrigerant leakage coupled with decreasing on-time apparently causes the PLF to drop below PLF levels observed for 2 min of extended indoor blower operation. However at 68% on-time, off cycle refrigerant migration control yields greater cycling COP improvements than that observed with extended indoor blower operation. Continuous operation of the indoor blower increased cycling degradations as compared to normal cycling mode operation for percent on-times less than 68%. At 20% on-time, heat delivered during the off cycle resulted in only a 21% degradation in steady state capacity (34% for normal mode); however, a 36% degradation in COP (16.9% for normal mode) was observed due to increased power consumption during the off cycle.

\* Compressor, indoor blower and outdoor fan cycle off during off cycle.

### LOSS PER CYCLE ANALYSIS

Normal mode cycling losses were compared to losses observed for cycling tests having off-cycle isolation of refrigerant in the indoor coil to reveal the underlying effects of refrigerant migration. Comparison of cycling transients were made for cycling tests having an 8-min-on and 30-min-off cycling rate conducted at an outdoor temperature of 50F (10°C).

Normalized capacity and compressor power, Figure 11, typify the improvement in part-load efficiency that results by isolating refrigerant within the condenser during the off-cycle. Air-side cycling capacity for the off-cycle refrigerant isolation test was observed to almost attain steady-state output, while for normal mode cycling operation capacity increased more gradually as discussed in the earlier section on cycling phenomena. No surge in compressor power was observed for the off-cycle refrigerant isolation test as seen in Figure 11. Power consumption, after the initial starting spike, increased steadily to near steady-state power levels; however, during normal mode cycling operation, the compressor power surged due to the high density of refrigerant entering the compressor at start-up. Also, since the majority of refrigerant was initially in the condenser, the evaporator did not become starved for refrigerant as occurs for normal mode cycling operation. A liquid seal indicating subcooling at the outdoor throttle was visually observed after 1 min of operation, in contrast to 3 min of operation for normal cycling operation. The differences in trends are again the result of start-up refrigerant dynamics that drastically affect compressor performance. Compressor housing temperature, measured at the compressor oil level, dropped 20F° (11C°) within 45 sec for normal mode cycling as compared to the gradual increase in housing temperature for the off cycle refrigerant isolation cycling test. The trends of compressor housing temperature in Figure 12 and compressor power in Figure 11 reveal the effects of start-up refrigerant dynamics on part load COP and capacity.

The analysis of losses per cycle, presented in Table 2 for the above cycling tests, shows cycling losses for refrigerant off-cycle isolation tests to be 40% less than cycling losses for normal mode operation. The change of indoor coil internal energy, comprised of coil thermal mass\* and refrigerant heat loss to coil and surroundings, was 12.6% of steady-state capacity for the isolation cycling test; however, for normal mode cycling, the internal energy loss from the indoor coil was 9.5% of steady-state capacity. Although the losses from the indoor heat exchanger ( $\Delta U_{HX}$ ) increased slightly with off-cycle isolation, a greater portion of hot refrigerant remains in the indoor coil and it can be utilized to improve cycling COP by extending indoor blower operation as previously discussed in the section on cycling control strategies. The loss due to refrigerant migration and start-up accumulator and compressor dynamics, termed refrigerant dynamic loss, was four times less for off cycle isolation of refrigerant as compared to normal mode cycling, Table 2. Again, the reduction of refrigerant dynamic loss during start-up occurs because of a reduction in the amount of liquid refrigerant entering the compressor and also a reduction in amount of refrigerant stored in the accumulator. These refrigerant transients within the compressor and accumulator prolong the system response time required to achieve steady-state operation. Increasing the size of the accumulator would decrease compressor power draw at start-up and thus improve part-load performance as observed by Tanaka (1982), but the cycling losses resulting from the need to establish proper charge distribution throughout the system would remain. Thus, best cycling performance clearly results by eliminating off-cycle refrigerant migration from the high-pressure side to the low-pressure side.

\* Product of coil metal mass, specific heat, and average coil wall temperature rise during the 8-min-on cycle.

## CONCLUSIONS

- Cycling COP and capacity degradations are inversely related to percent on-time. As length of off cycle increases (decreasing % on-time), the time required to reestablish condenser and evaporator steady-state operating conditions, proper refrigerant charge distribution, and equilibrium temperatures in the thermal mass of the system increases.
- Analysis of capacity loss per cycle, for tests having cycling rates of 8-min-on and 30-min-off, showed the major cycling loss to be due to off cycle refrigerant migration and its effect on the compressor in achieving steady-state operation after start-up.
- The ratio of part-load COP to steady-state COP (PLF) is dependent on outdoor temperature. The cycling losses decrease with decreasing outdoor temperature because refrigerant density effects result in less refrigerant circulating throughout the system; therefore, less time is required to achieve proper steady-state charge distribution.
- The control of off-cycle refrigerant migration and extending indoor blower operation by 2 min yields an 11% improvement in part-load capacity as contrasted to normal mode cycling capacity.

## REFERENCES

- Kelly, George E.; and Parken, Walter H. 1977. "Factors affecting the performance of a residential air-to-air heat pump." ASHRAE Transactions Part 1, pp. 839-849.
- Tanaka, N.; and Yamanaka, G. 1982. "Experimental study on the dynamic characteristics of a heat pump" ASHRAE Transactions 88, Part 2, pp. 323-331.
- Mulroy, William J.; and Didion, David A. 1983. "A laboratory investigation of refrigerant migration in a split unit air conditioner." NBSIR 83-2756. U.S. Department of Commerce, National Bureau of Standards.
- Murphy, W. E.; and Goldschmidt, V. W. 1984. "Transient response of air conditioners - A qualitative interpretation through a sample case." ASHRAE Transactions 90, Part 1B, pp. 997-1008.
- Energy Conservation Program for Consumer Products: 1979. "Test procedures for central air conditioners, including heat pumps." Federal Register, DOE 10 CFR, Part 44, Vol. 249.
- Baxter, V. D.; and Moyers, J. C. 1984. "Air source heat pump: field measurements of cycling frosting and defrosting losses, 1981-1983." ORNL/CON-150. Oak Ridge, TN: Oak Ridge National Laboratory, November.
- Lamb, G.; and Tree, David R. 1981. "Seasonal performance of air conditioners -- an analysis of the DOE test procedure: the thermostat and measurement errors." DOE/CS/23337-2, National Technical Information Service.
- Mulroy, William J.; and Didion, David A. 1985. "Refrigerant migration in a split-unit air conditioner." ASHRAE Transactions Part 1A, pp. 193-206.

## ACKNOWLEDGMENT

This research was sponsored by the Office of Buildings Equipment Research and Development, U.S. Department of Energy, under contract DE-AC05-84OR21400 with Martin Marietta Energy Systems, Inc.

TABLE 1  
Steady-State Charge Distribution

Heat Pump Section	Refrigerant Weight lb (kg)	
	50F (10°C)	30F (-1°C)
Outdoor Unit	4.3 (1.9)	6.7 (3.9) ← 3.0
Indoor HX	6.0 (2.7)	3.6 (1.6)
Liquid Line	1.9 (.88)	1.9 (.88)
Vapor Line	.27 (.12)	.19 (.09)
	12.47	12.39

TABLE 2  
Loss Analysis for Tests Having an 8-min-on and 30-min-off  
Cycling Rate Observed at 10°C (50°F) Outdoor Temperature

	$Q_{LOSS/CYC}^{(A)}$ Btu (wh)	$\frac{\Delta U_{HX}}{Q_{REF}^{(C)}}$ $Q_{LOSS}^{(B)}$ % of $(Q_{in}) (T_{in})$		$Q_{REF,DYN}^{(D)}$	TOTAL
		$Q_{LOSS}^{(B)}$	$Q_{REF}^{(C)}$		
Compressor and Fans Cycle On/Off	1254. (367.)	5.5	4.05	19.34	28.9
Refrigerant Isolated <sup>(E)</sup> in indoor HX during off cycle	809.5 (237.)	6.3	6.3	5.1	17.6

<sup>A</sup> Loss calculated over 8 min on period based on air side measurements.

<sup>B</sup> Thermal mass loss of indoor coil metal equated to product of coil metal thermal mass and coil temperature gain during on cycle.

<sup>C</sup> Refrigerant energy loss to indoor coil and surroundings during off cycle using first law analysis.

<sup>D</sup> Refrigerant heat loss due to migration and compressor, accumulator start-up refrigerant transients.

<sup>E</sup> Isolation valves in liquid and vapor lines leaked 1.8 lb (0.8 kg) of refrigerant during 30 min off cycle.

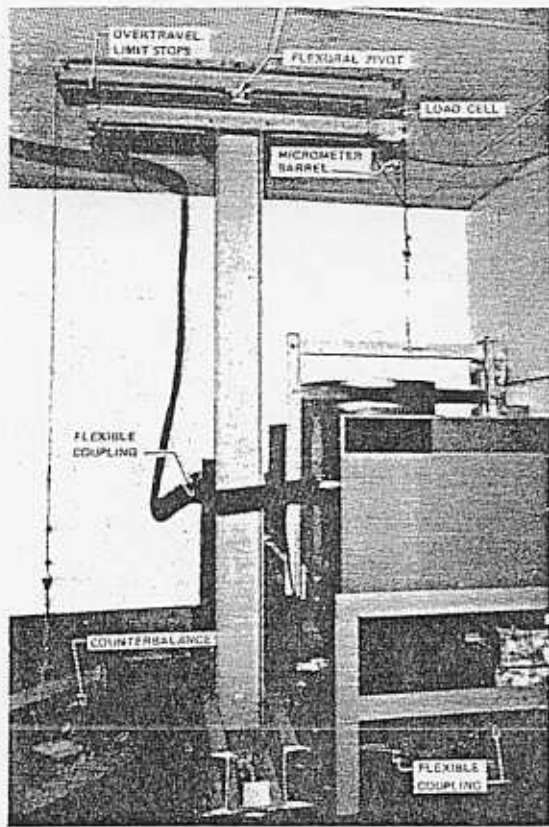


Figure 1. Weighing system for measurement of refrigerant weight in outdoor unit

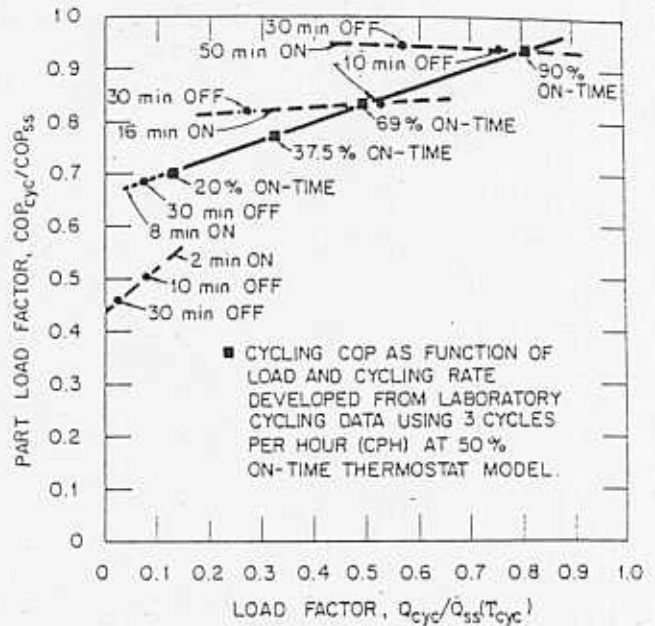


Figure 2. Heat pump cycling performance observed at 50 F (10°C) outdoor temperature

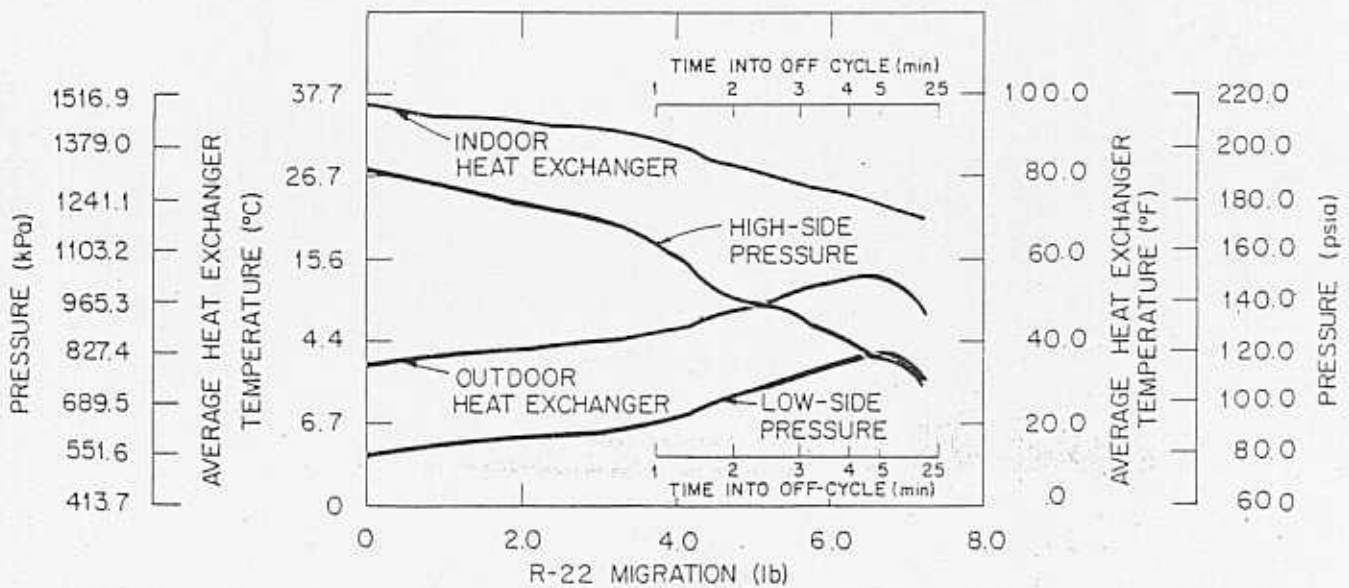


Figure 3. Average heat exchanger temperature and refrigerant pressure plotted as function of refrigerant migration to the outdoor unit during the off cycle of an 8-min-on and 30-min-off cycling test conducted at 50 F (10°C) outdoor temperature

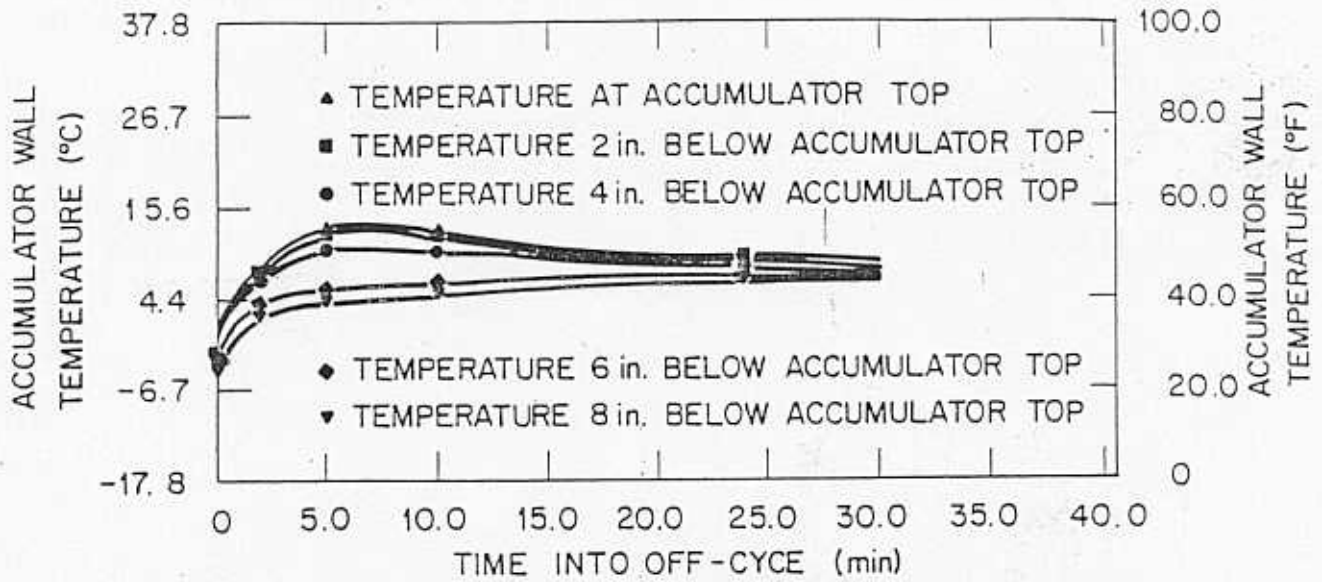


Figure 4. Accumulator wall temperatures observed during the off cycle of an 8-min-on and 30-min-off cycling test conducted at 50 F (10°C) outdoor temperature

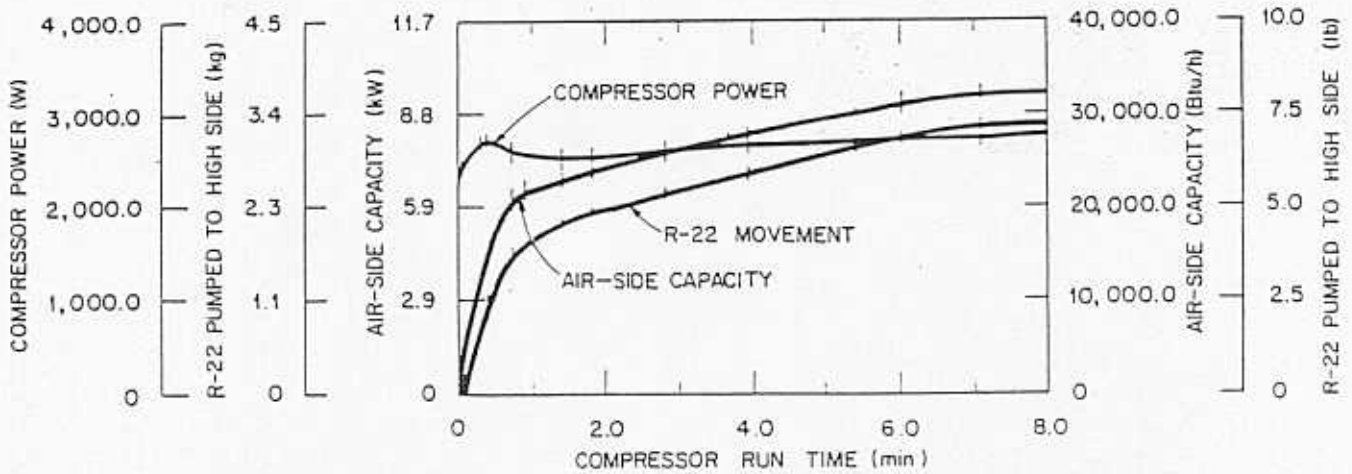


Figure 5. Capacity, compressor power, and refrigerant pumped to high side during the on period of an 8-min-on and 30-min-off cycling test conducted at 50 F (10°C) outdoor temperature

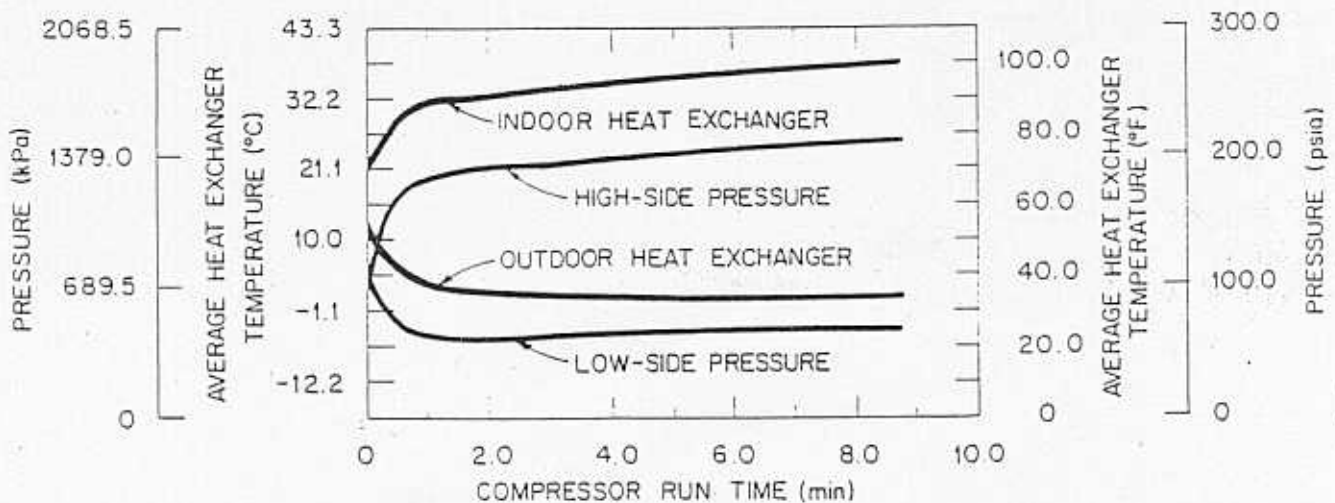


Figure 6. Average heat exchanger temperature and refrigerant pressure measured during the on period of an 8-min-on and 30-min-off cycling test conducted at 50 F (10°C) outdoor temperature

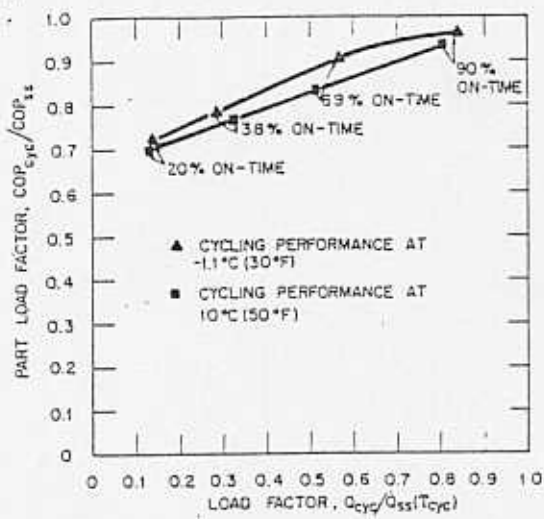


Figure 7. Outdoor temperature effect on heat pump cycling COP

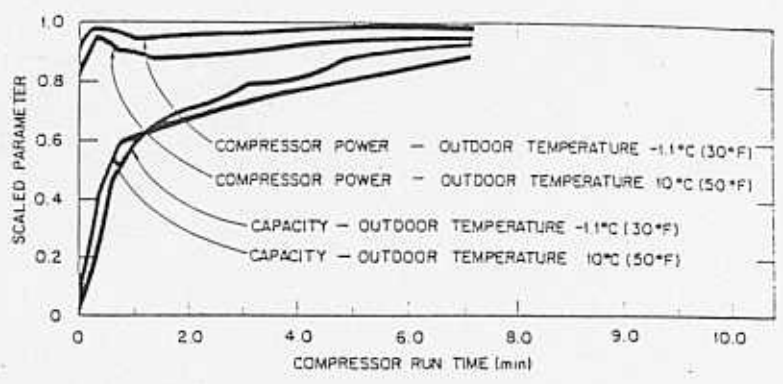


Figure 8. Capacity and compressor power, normalized to steady-state value, for the one period of 8-min-on and 30-min-off cycling tests

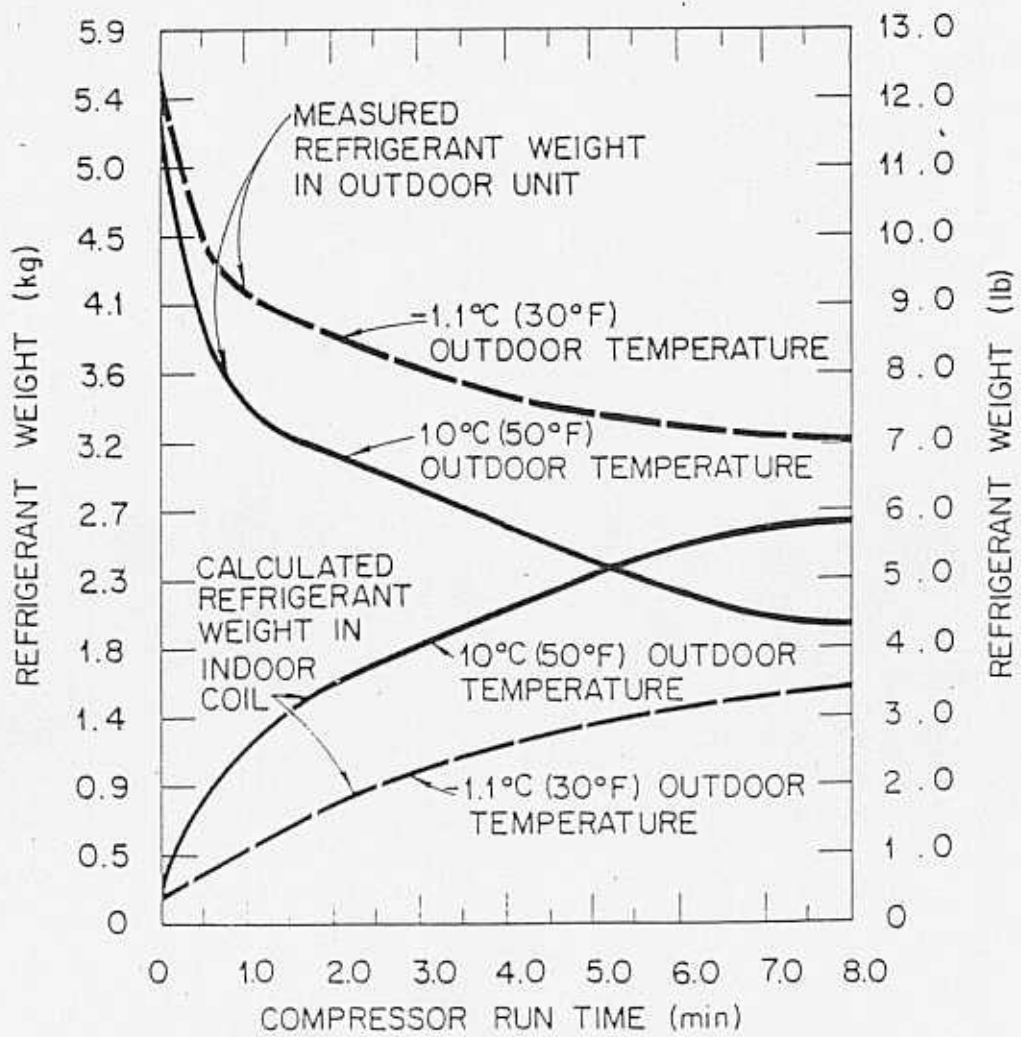


Figure 9. On period charge distribution as affected by outdoor temperature for cycling tests having 8-min-on and 30-min-off cycling rate

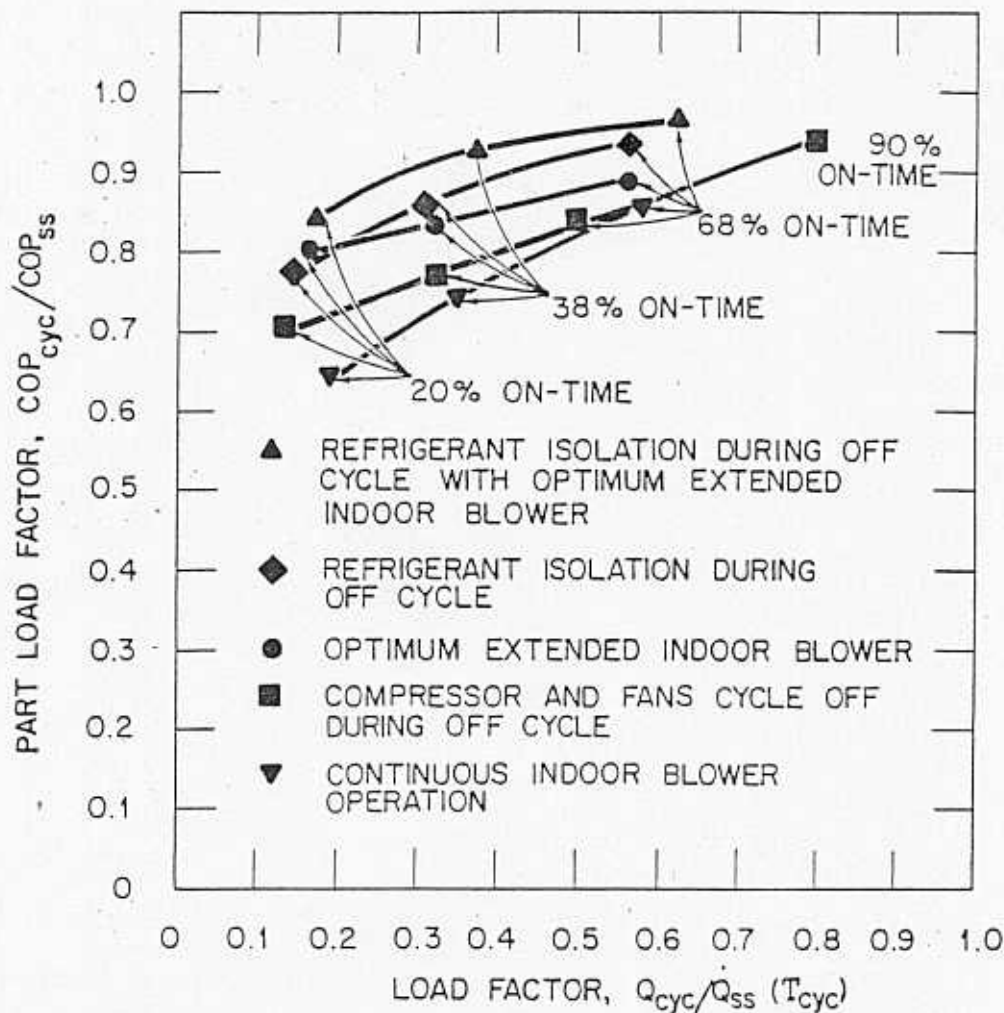


Figure 10. Heat pump heating mode cycling COP observed at 50 F (10°C) outdoor temperature for various cycling control strategies

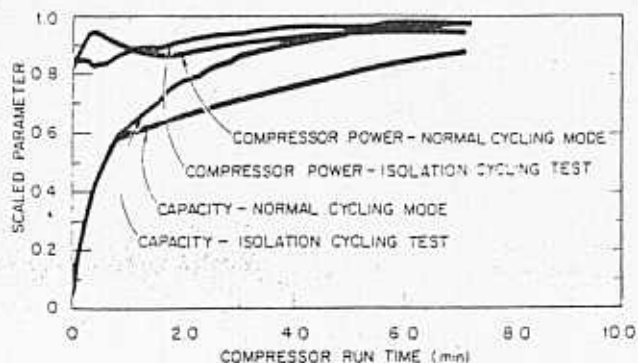


Figure 11. Capacity and compressor power, normalized to steady-state, for comparison of normal mode cycling to cycling with off cycle isolation of refrigerant in the indoor coil

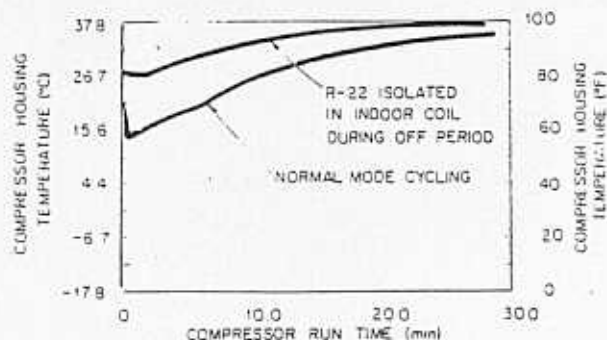


Figure 12. Compressor housing temperature, measured at compressor oil level, for cycling tests having off cycle refrigerant migration control and normal mode control